Controlling films structure by regulating 2D Ruddlesden-Popper perovskite formation enthalpy for efficient and stable tri-cation perovskite solar cells

Chao Liang,‡[a] K. M. Muhammed Salim,‡[b] Pengwei Li,‡[c] Zhuo Wang,[d] Teck Ming Koh,[b] Hao Gu,[a] Bo Wu,[e] Junmin Xia,[a] Zhipeng Zhang,[a] Kaiyang Wang,[a] Tanghao Liu,[a] Qi Wei,[a] Sisi Wang,[a] Yuxin Tang,[a] Guosheng Shao,[d] Yanlin Song,[c] Nripan Mathews[b] and Guichuan Xing*[a]*

[a]Joint Key Laboratory of the Ministry of Education, Institute of Applied Physics and Materials Engineering, University of Macau, Avenida da Universidade, Taipa, Macau 999078, P. R. China.

[b]Energy Research Institute @ NTU (ERI@N), Research Techno Plaza, X-Frontier Block, Level 5, 50 Nanyang Drive, 637553, Singapore.

[c]Key Laboratory of Green Printing, Institute of Chemistry, Chinese Academy of Sciences (ICCAS), Beijing Engineering Research Center of Nanomaterials for Green Printing Technology, Beijing National Laboratory for Molecular Sciences (BNLMS), Beijing 100190, P. R. China.

[d]State Centre for International Cooperation on Designer Low-Carbon and Environmental Material (SCICDLCEM), School of Materials Science and Engineering, Zhengzhou University, Zhengzhou 450001, P. R. China.

[e]Guangdong Provincial Key Laboratory of Optical Information Materials and Technology & Institute of Electronic Paper Displays, South China Academy of Advanced Optoelectronics, South China Normal University, Guangzhou 510006, P. R. China.

Corresponding Author

*E-mail: Nripan@ntu.edu.sg (N. Mathews) and gcxing@um.edu.mo (G. Xing)

‡C. Liang, K. M. M. Salim and P. Li contributed equally to this work.

Experimental Section

Materials: Cesium iodide (CsI), Formamidinium iodide (FAI), methylammonium bromine (MABr), methylammonium iodide (MAI), Lead iodide (PbI_2), lead bromine ($PbBr_2$), 4-tert-butylpyridine (t-BP), lithium-bis(tri-fluoromethanesulfonyl)imide (Li-TFSI) and 2,2,7,7-tetrakis(N,N-di-pmethoxyphenylamine)-9,9-spirobifluorene (spiro-MeOTAD) were purchased from Xi'an Polymer Light Technology Corp. The SnO_2 colloidal dispersion and all anhydrous solvents were purchased from Alfa–Aesar.

$CF_3CF_2CH_2NH_3I$ (5F-PAI): 0.9 mL of hydroiodic acid (57 wt% in water) was dropped into a solution containing 1 g of pentafluoropropyl ammonium (TCI) in methanol which was previously cooled to 0 ^oC. The amine to hydroiodic acid ratio is kept at 1:1.01. The solution was stirred for 8 h. A concentrated pale-yellow solution was obtained by rotavapor and redissolved with a minimum amount of ethanol and prior to re-precipitation in diethyl ether. The solid was then dried under vacuum for 1 day at 50 ^oC.

Fabrication of PSCs: Indium tin oxide (ITO) were cleaned by sequentially sonication in DI water, acetone, and IPA. Then, the ITO were treated under UVO for 20 min. The as purchased SnO_2 was diluted by water (1:2 wt), and then spin-coated onto the clean ITO/glass at 3000 rpm for 30s. The film was dried at 150 °C for 30 min. The 5F-$PA_x[Cs_{0.05}(FA_{0.83}MA_{0.17})_{0.95}]_{1-x}Pb(I_{0.83}Br_{0.17})_3$ precursor solution was prepared by dissolving 183 mg FAI, 514 mg PbI_2, 24 mg MABr, 86 mg $PbBr_2$, 45μL CsI (1.5 M in DMSO) and the proportionate 5F-PAI in 0.8 mL DMF and 0.2 mL DMSO. The perovskite layer was obtained using a two steps program at 2000 and 6000 rpm for 15 and 25 s. 150 μL chlorobenzene was dripped 10 s before the process ended and this was

followed by annealing at 110 °C for 30 min. The spiro-MeOTAD (72.3 mg in chlorobenzene) was spin coated at 3500 r.p.m. for 25 s. Spiro-MeOTAD was doped with 28.8 mL t-BP, and 17.5 mL Li-TFSI (520 mg mL^{-1} in acetonitrile). Finally, 80 nm gold electrode was evaporated.

Characterization: Crystal phase information was studied by a Rigaku X-ray di□raction (Cu target radiation source, λ=1.54 Å). And the absorption spectra were measured by a UV-2550 spectrophotometer. The PL spectra were collected by Edinburgh Instruments (FLSP920). SEM images were collected by a field-emission scanning electron microscope (J-7500F). IPCE was obtained by a Newport IPCE system. The J-V curves were obtained employing a Keithley 2400 source meter and AM1.5G simulated illumination (100mW/cm^2, Newport). TRPL was obtained by using an HAMAMATSU™ streak camera system with an ~1 ps temporal resolution. For stability measurement, all of the solar cells were aged under open-circuit conditions. No additional ultraviolet filter was employed during the ageing process.

Transient absorption: The TA spectra were measured by employing the HELIOS TA system. The laser source was the Coherent Legend regenerative amplifier (150 fs, 1 KHz, 800 nm) seeded by a Coherent Vitesse oscillator (100 fs, 80 MHz). A small portion (around 10 mJ) of the laser fundamental 800 nm laser pulses was focused into a sapphire plate to produce broadband probe pulses in the visible region. In addition, the TOPAS-C optical parametric amplifier generated a 425-nm pump pulses.

DFT simulation: These ΔH_f, are estimated via

$$2\ \text{nF-PAI} + 2\ \text{MAI} + 3\ PbI_2 \rightarrow \text{nF-}PA_2MA_2Pb_3I_{10}$$

The structures of nF-$PA_2MA_2Pb_3I_{10}$ (detailed in Table S1), MAI, PbI_2 and nF-PAI are built according to ref.S1 and have been fully optimized during the simulation.

S1 J. M. Hoffman, X. Che, S. Sidhik, X. Li, I. Hadar, J. Blancon, H. Yamaguchi, M. Kepenekian, C. Katan, J. Even, C. C. Stoumpos, A. D. Mohite, M. G. Kanatzidis, *J. Am. Chem. Soc.*, 2019, **141**, 27, 10661-10676.

Table S1. Structure refinement for $PA_2MA_2Pb_3I_{10}$.

Empirical formula	$C_8N_4H_{32}Pb_3I_{10}$
Cell setting	Monoclinic
Space group	P21/c
a/Å	8.85
b/Å	25.628
c/Å	8.85
α/°	90
β/°	103.593
γ /°	90
Volume / $Å^3$	1967.8225

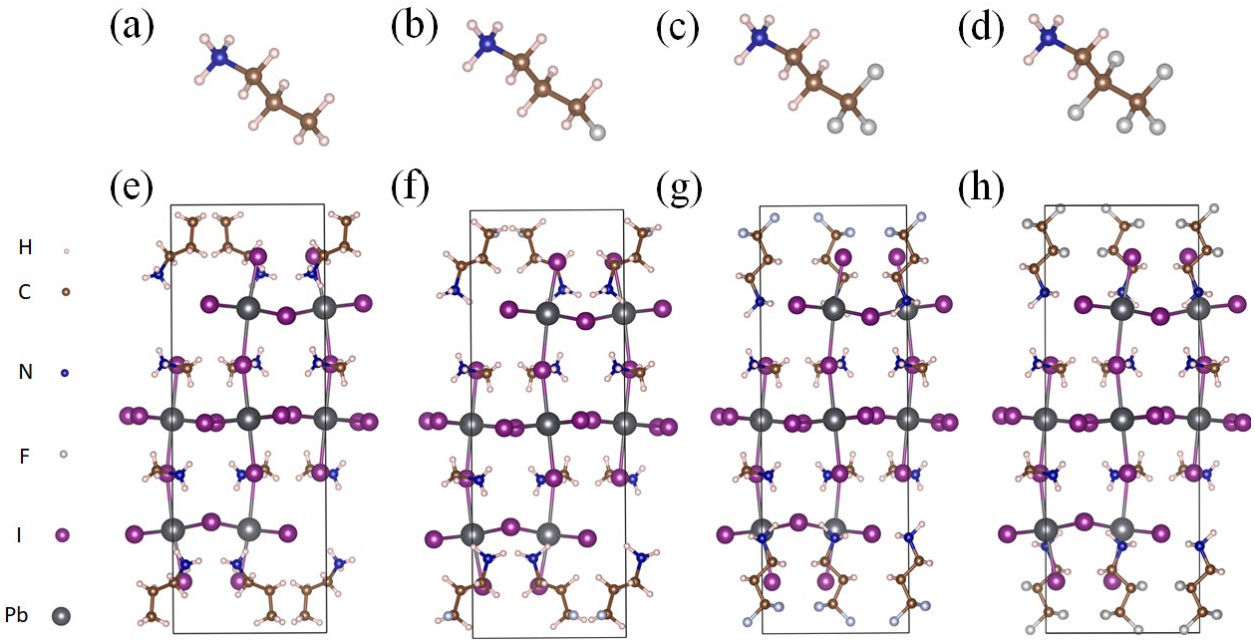

Fig. S1. The molecular structures of the (a) PA^+, (b) 1F-PA^+, (c) 3F-PA^+, (d) 5F-PA^+, (e) $PA_2MA_2Pb_3I_{10}$, 1F-$PA_2MA_2Pb_3I_{10}$, 3F-$PA_2MA_2Pb_3I_{10}$ and 5F-$PA_2MA_2Pb_3I_{10}$.

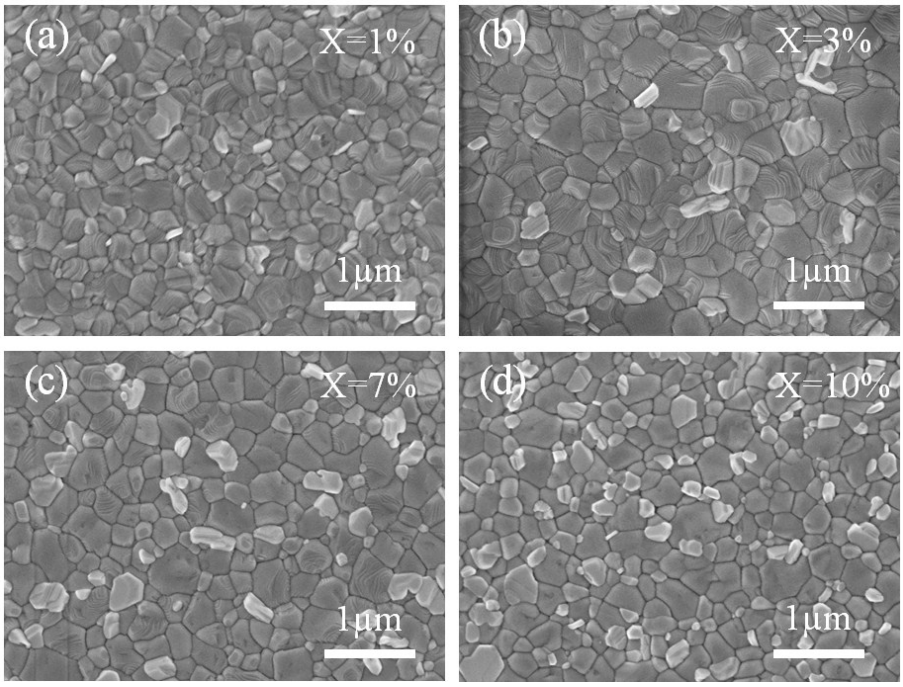

Fig. S2. Top-view scanning electron microscopy (SEM) images of the 5F-PAI incorporated perovskite with different 5F-PAI ratio.

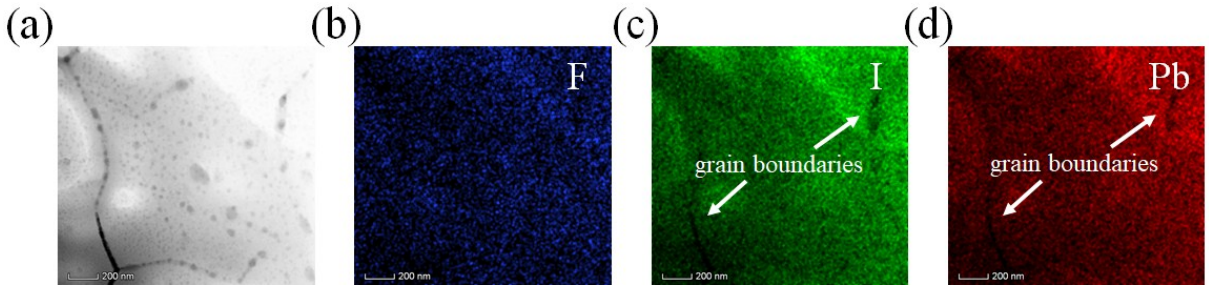

Fig. S3. (a) Low-resolution Transmission Electron Microscopic (TEM) images of 5% 5F-PAI-incorporated perovskite and (b-d) corresponding EDX mapping images of F, I and Pb.

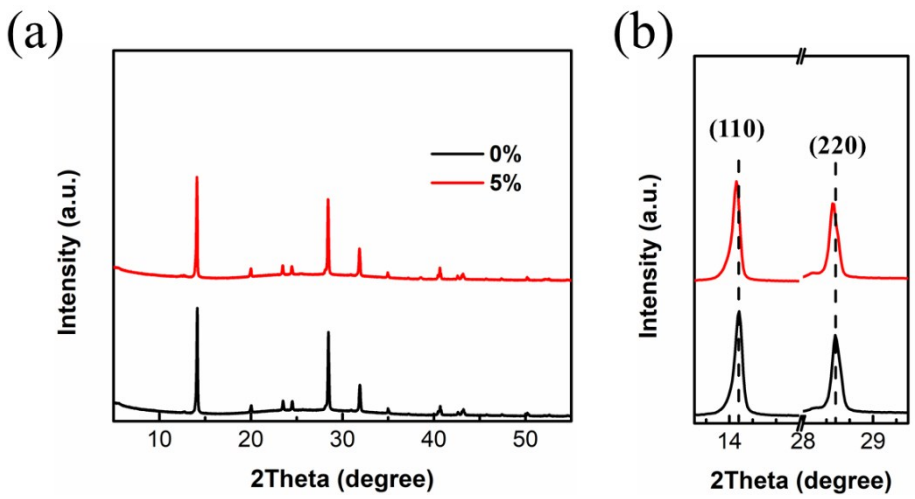

Fig. S4. (a) X-Ray diffraction (XRD) pattern and (b) Magnification of (110) and (220) peaks of the pristine perovskite and 5% PAI-incorporated perovskite.

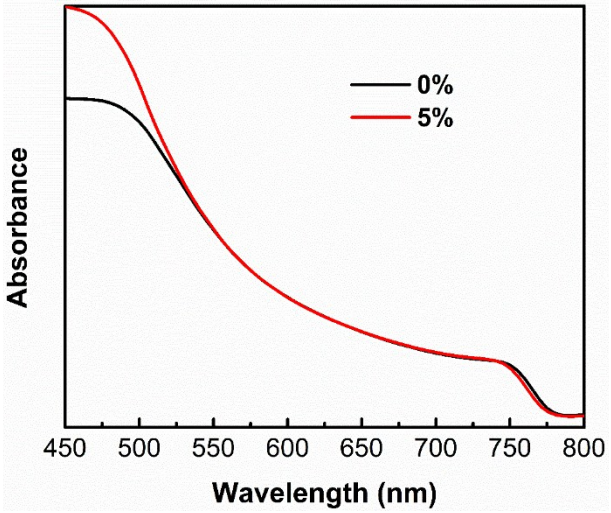

Fig. S5. Absorption spectra of the control perovskite and 5% PAI-incorporated perovskite.

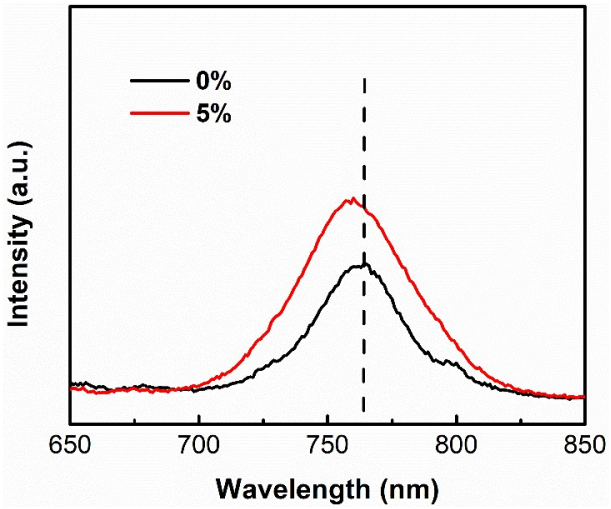

Fig. S6. PL spectra of the pristine perovskite and 5% PAI-incorporated perovskite.

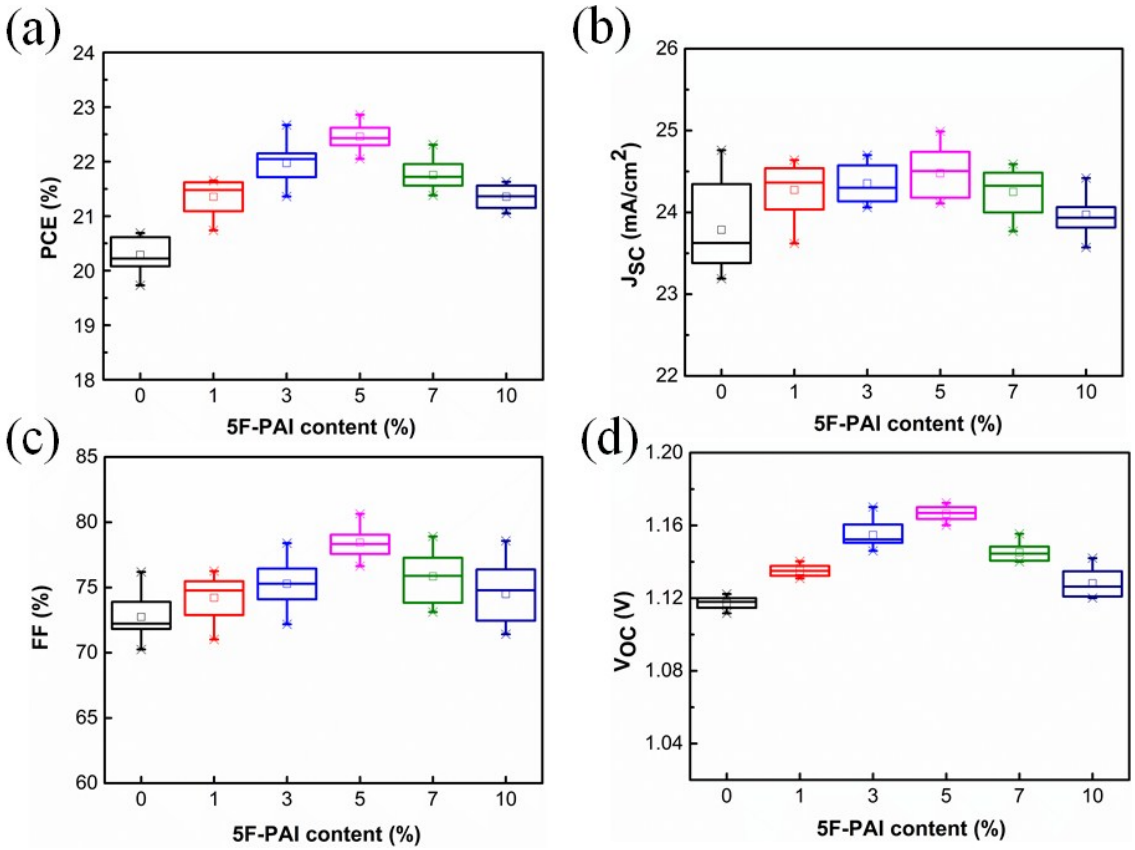

Fig. S7. (a-d) Statistical data for *PCE*, J_{SC}, *FF* and V_{OC} from 20 cells per condition.

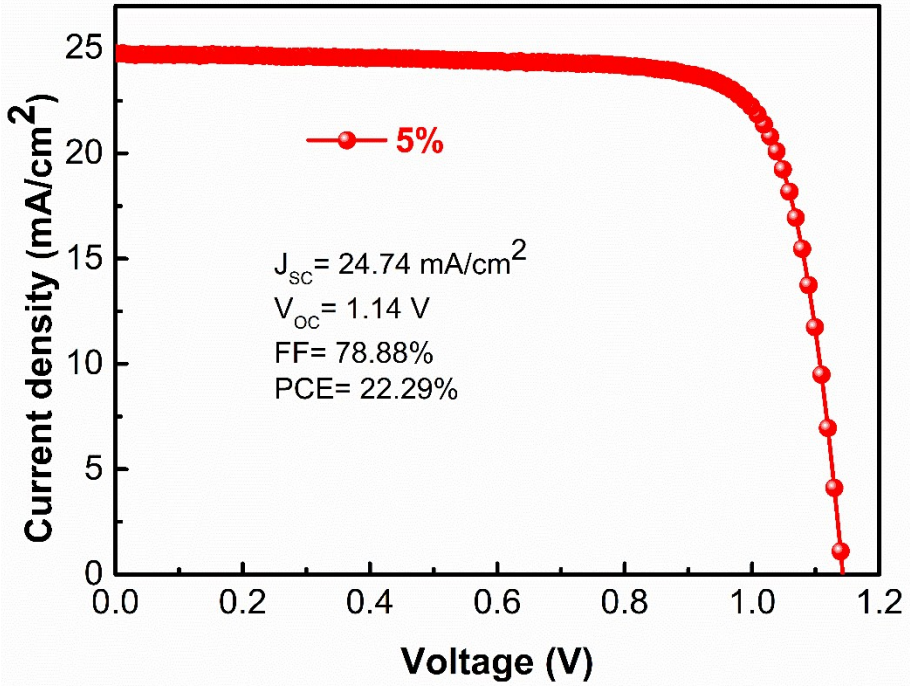

Fig. S8. J–V curves of champion devices by employing PAI cation.

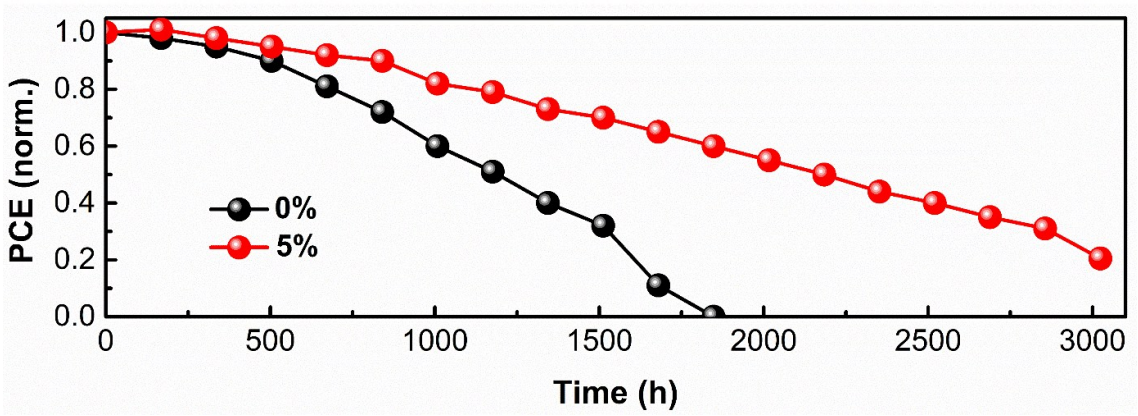

Fig. S9. Stability test of devices using pristine perovskite and 5% PAI-incorporated perovskite under dark with 65±10% humidity.

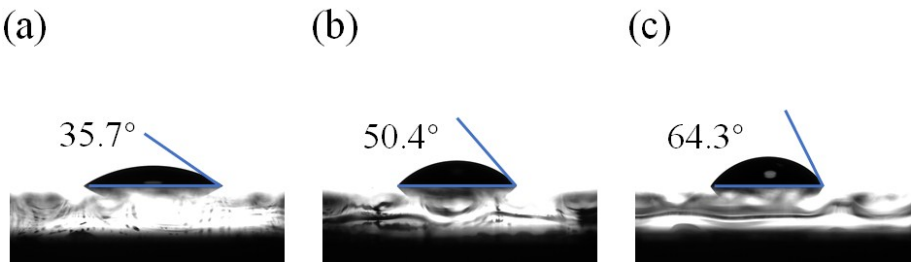

Fig. S10. Contact angle of water on (a) pristine perovskite films, (b) 5% PAI-incorporated perovskite films and (c) 5% 5F-PAI-incorporated perovskite films.

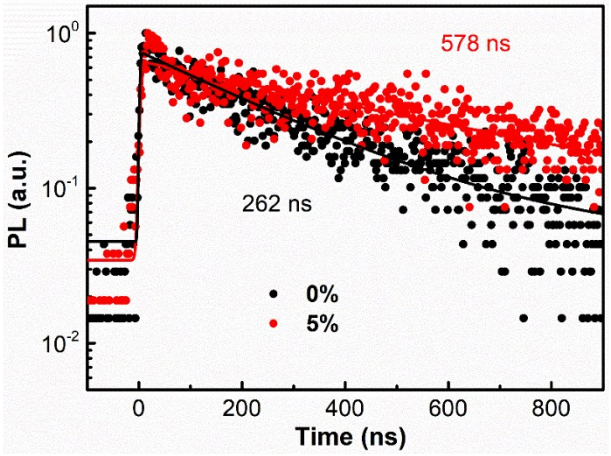

Fig. S11. TRPL decay curves of pristine perovskite and 5% PAI-incorporated perovskite films.

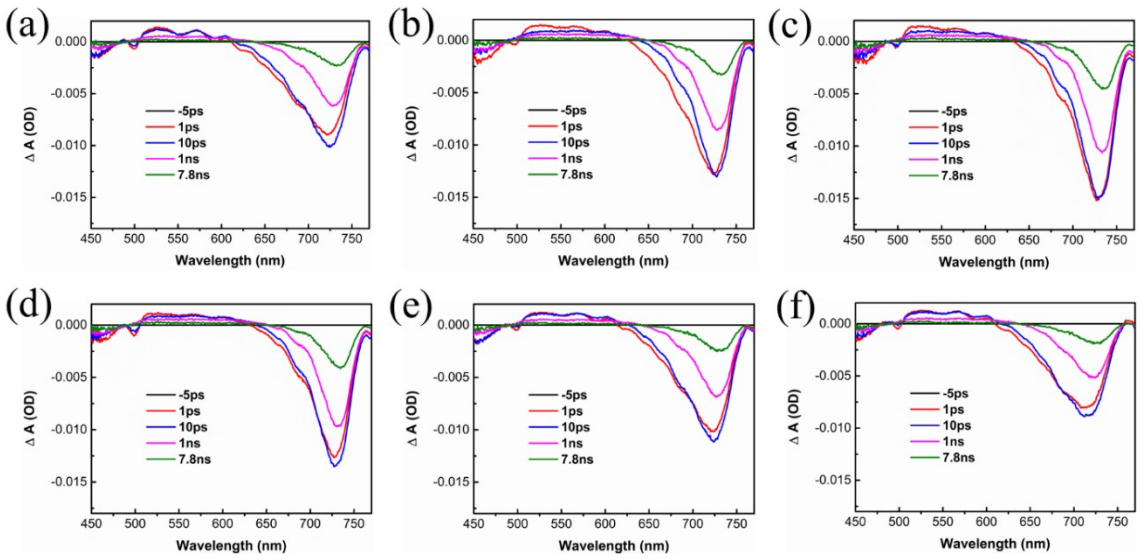

Fig. S12. TA spectroscopy of pristine perovskite (a) and 5F-PAI incorporated perovskite with different 5F-PAI concentrations (1% (b), 3% (c), 5% (d), 7% (e) and 10% (f)) films following excitation at 425 nm (~1 μJ/cm^2).

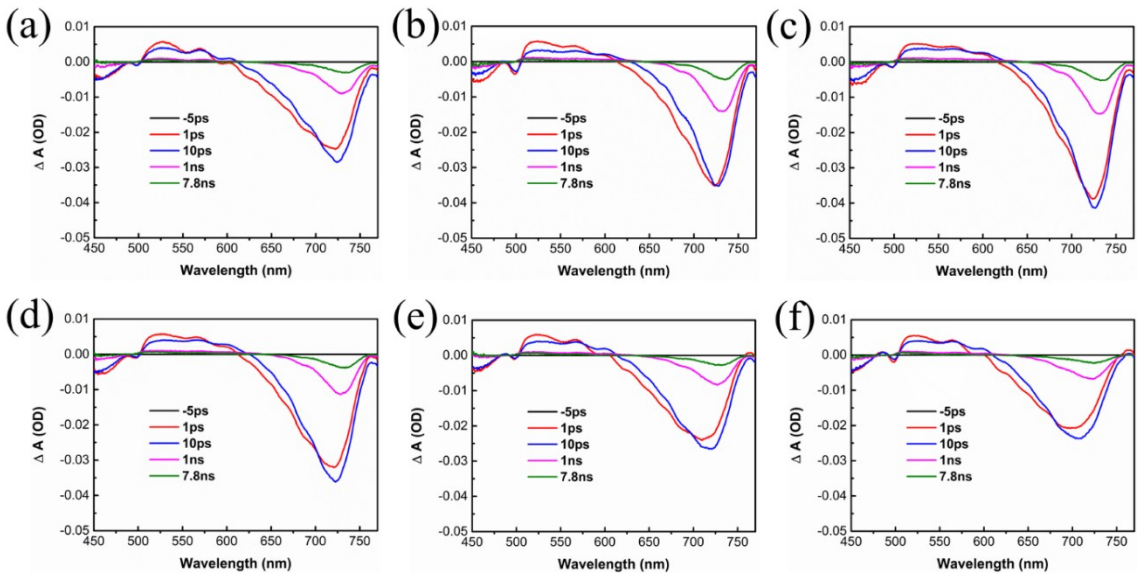

Fig. S13. TA spectroscopy of pristine perovskite (a) and 5F-PAI incorporated perovskite with different 5F-PAI concentrations (1% (b), 3% (c), 5% (d), 7% (e) and 10% (f)) following excitation at 425 nm (~2 μJ/cm^2).

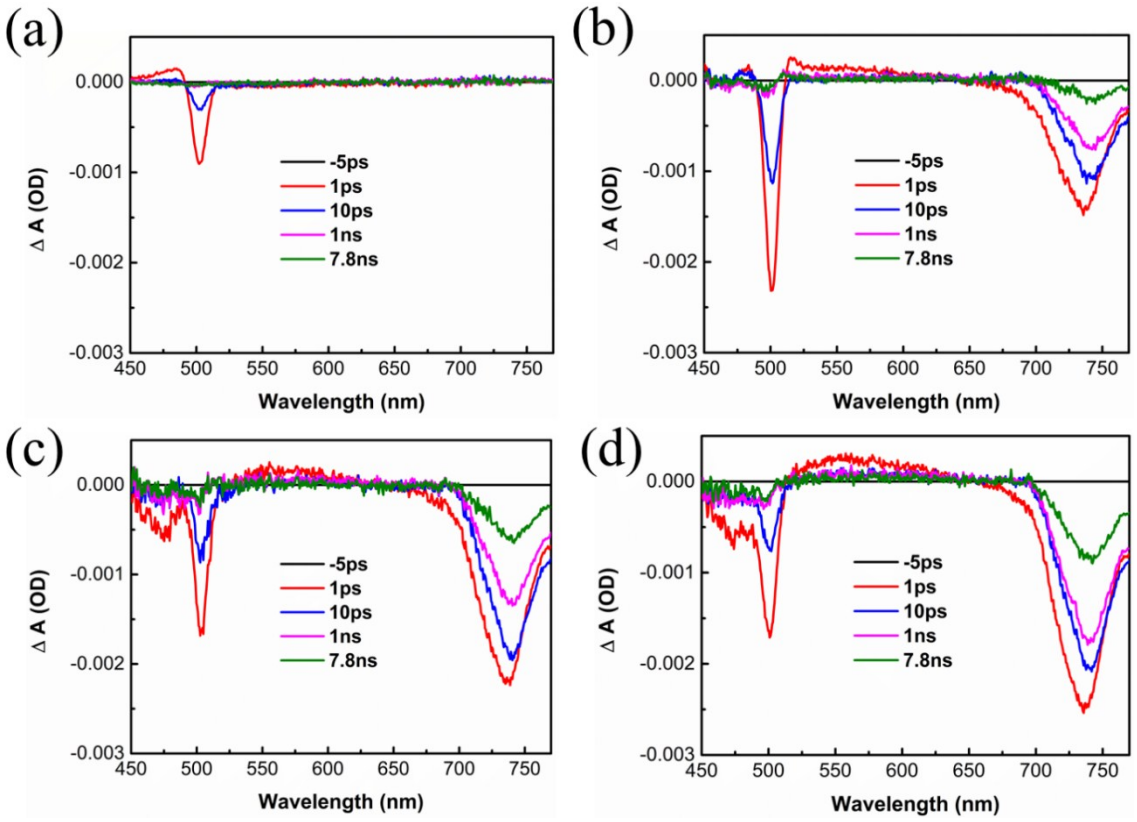

Fig. S14. a-d) TA spectroscopy of high-concentration 5F-PAI incorporated perovskite with different 5F-PAI concentrations films (5F-$PA_2MA_{n-1}Pb_nI_{3n+1}$, n=1, 2, 3, 4), respectively, at selected probe delay times following excitation at 425 nm (~0.8 μJ/cm^2).

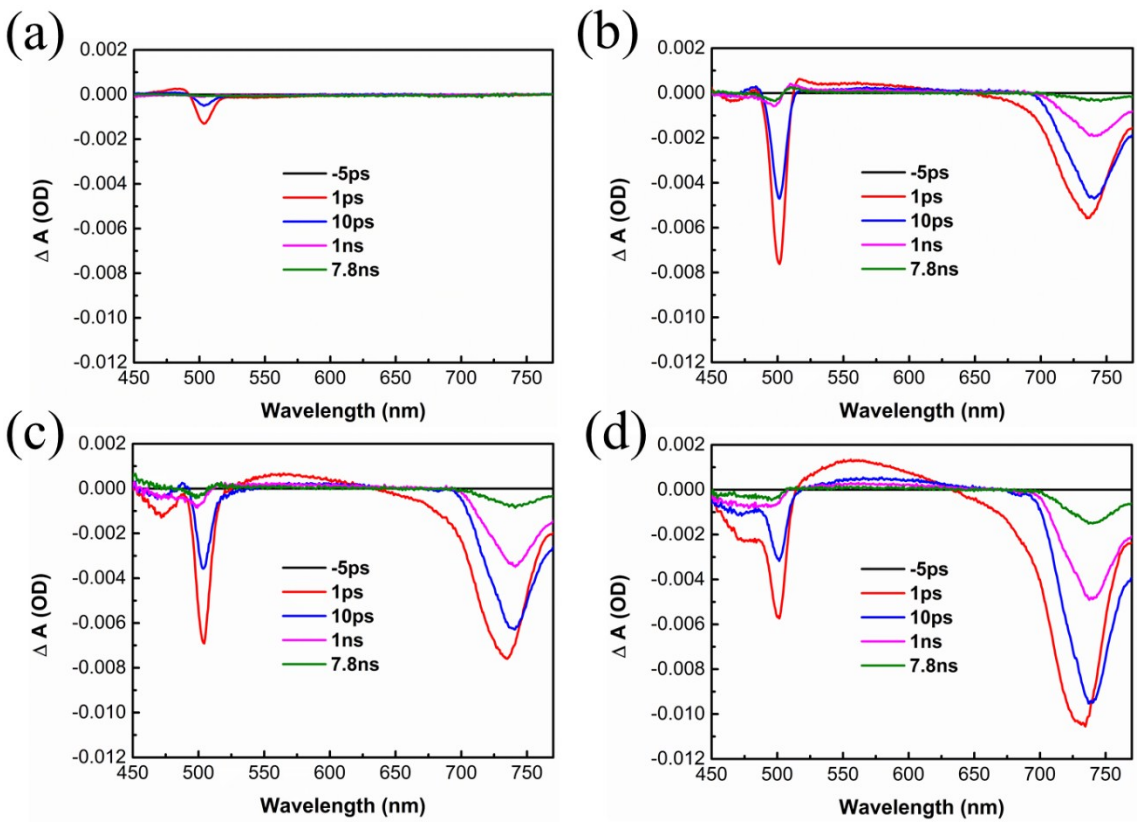

Fig. S15. a-d) TA spectroscopy of high-concentration 5F-PAI incorporated perovskite with different 5F-PAI concentrations films (5F-$PA_2MA_{n-1}Pb_nI_{3n+1}$, n=1, 2, 3, 4), respectively, at selected probe delay times following excitation at 425 nm (~1.6 μJ/cm^2).

Table S2. The detailed parameter of devices by using 5F-$PA_x[Cs_{0.05}(FA_{0.83}MA_{0.17})_{0.95}]_{1-x}Pb(I_{0.83}Br_{0.17})_3$.

PFPA (%)	J_{SC} (mA/cm^2)	V_{OC} (V)	*FF* (%)	*PCE* (%)
0	24.76	1.13	74.00	20.69
1	24.64	1.14	76.88	21.65
3	24.70	1.17	78.46	22.67
5	24.57	1.17	79.15	22.86
7	24.80	1.14	78.68	22.31
10	24.72	1.14	76.53	21.63

Table S3. The detailed photovoltaic parameters of devices using the pristine perovskite and 5% 5F-PAI-incorporated perovskite.

PFPA (%)	Scan direction	J_{SC} (mA/cm^2)	V_{OC} (V)	*FF* (%)	*PCE* (%)
0	Forward	24.64	1.13	70.77	19.75
0	Reverse	24.76	1.13	74.00	20.69
5	Forward	24.51	1.17	78.76	22.62
5	Reverse	24.57	1.17	79.15	22.86